Glide Processes of a Snow Cover as a Release Mechanism of an Avalanche on a Slope Covered with Bamboo Bushes*

by

Yasoichi ENDO
遠 藤 八十一
The Institute of Low Temperature Science

Received December 1983

Abstract

Based on several winters' observations of a snow cover on a slope covered with bamboos, a unified explanation of the behavior of the snow cover until the release of a full-depth slab avalanche was given in terms of the glide of snow, where the friction of the slope, or more precisely, the momentum exchange of the snow cover and the slope, was shown to be composed of the resistance of the bamboos standing entrapped *in* snow and that of those lying flat *under* snow. Simulated experiments gave the former as a function of glide speed and glide distance as well as the latter as a function of glide speed. Using these functions, the behavior of a snow mass on a uniform slope was quantitatively discussed. Finally, the distribution of stress and that of glide speed in a region of the snow cover, where the snow is supported mainly by surrounding snow, were numerically computed.

* Contribution No. 2626 from the Institute of Low Temperature Science
北海道大学審査学位論文

Contents

I. Introduction

Snow avalanches are divided into two groups by the modes of release : "loose snow avalanches" and "slab avalanches" (The Japanese Society of Snow and Ice, 1964). The former start from a point of a snow cover near the surface and propagate downhill by dislodging successively downstream parts of loose snow. Despite frequent occurrence, they are usually limited in extension and innocuous as well. Meanwhile, the latter come about from the sudden falling of an extensive area of a snow cover resulting in the release of a coherent mass of snow. Severe damage is mailnly caused by them. The slab avalanches are further divided into two subgroups : The one is "surface slab avalanches" in which only an upper layer of the snow cover falls. The other is "full-depth slab avalanches" in which the whole snow cover falls, occurring in Japan mostly on slopes covered with light vegetation such as bamboo bushes and tall grasses. This paper will treat on processes from the formation of a snow cover on a slope covered with bamboo bushes to the release of a full-depth slab avalanche.

Now, the release mechanism of a full-depth avalanche is understood as follows : Consider a snow mass on a uniform slope. The mass will be said to be "stable at the bottom" when the driving force of the mass, namely, the component of the gravity force on it along the slope, is balanced by friction between the mass and the slope. In this case, the mass will glide down with a constant speed over the slope. But if it becomes unstable at the bottom, the speed will accelerate uncontrollably, or in other words, an avalanche breaks out. When only a part of a snow cover becomes unstable, however, an avalanche will not always occur immediately, because the snow cover may have such an additional support of the surrounding snow mass that an avalanche will start only after the loss of the support as a result of the fracture of snow at a boundary with the surrounding snow mass. Thus the primary condition for the release of a full-depth slab avalanche is the loss of stability at the bottom of a snow cover in an extended area, and the secondary condition or the trigger is the fracture of snow at the boundary of the area.

Hitherto, it has been considered that the primary condition is contributed to by changes in snow properties such as increase in free water content, formation of a depth-hoar layer, and so on, while the secondary condition by spatial differences of snow glide (U. S. Forest Service, 1961 ; Mellor, 1968). From such a viewpoint, measurements of snow glide have been conducted by many researchers including the author (in der Gand and Zupacic, 1966 ; Akitaya, 1974, 1975 ; McClang, 1975 ; Endo and Akitaya, 1976 ; Yamada, 1977). Some of them suspected that the glide may also contribute to the primary condition. However, no clear evidence has been offered concerning it.

The present paper will validate, as a conclusion, the existence of such a contribution for most of the observed full-depth slab avalanches, and try to describe, in terms of the snow

glide, the whole processes leading to the release of an avalanche on a slope covered with bamboo bushes.

In this connection, Chapter II will be devoted to describing observed facts from which the above conclusion has been derived. Particularly, it is shown that friction at the bottom of a snow cover can be considered to be composed of the resistance of bamboos remaining entrapped in the snow cover and that of bamboos falling down flat under snow and thus covering the slope. Next, Chapter III will show that each resistance depends both on glide speed and glide distance and that the value of resistance is quantitatively obtained from the results of simulated laboratory experiments. Then, Chapter IV will treat on the analysis of the behavior of a snow mass on a uniform slope using the relations obtained in Chapter III. Finally, Chapter V will give the distributions of stress and glide speed in an area of a snow cover when the only unstable area is the bottom. These distributions allow us to compute the values of maximum tensile stress and maximum glide speed immediately before a crack is formed in observed cases ; from these maximum values a criterion for the formation of a crack is given. It turns out, then, that the criterion is given only in terms of the maximum glide speed, which is not difficult to obtain.

II. Field observations of snow gliding on a slope covered with bamboo bushes

II. 1 *Terrain and climate*

The south slope of a ridge in the Teshio District, Hokkaido, was subjected to measurements of snow glide and observations of phenomena accompanied, the ridge being the site of the Avalanche Observatory of the Institute of Low Temperature Science, Hokkaido University. The slope is almost uniformly inclined at 30 to 35° and is covered only with dwarf bamboo bushes 0.8 to 1.0 m high. Number density of bamboo stands is 70 to 100 per square meter. Every year sees avalanches occurring on this south slope in large numbers, but none on the north slope of the same ridge which abound in large trees.

On the south slope a seasonal snow cover usually forms in early December and disappears by early April. Yearly maximum snow depth ranges between 1.0 and 1.5 m. Mean density of the snow cover is about 300 kg/m^3. Monthly mean air temperatures of January and February are about -7 to -8°C. Air temperature rises above 0°C seldom in these months but often in March. Under normal snowfall conditions, snow temperature is 0°C at the bottom of the snow cover throughout the winter and varies from -1 to -3°C at 0.3 m above it.

II. 2 *Method of glide measurement*

Measurements were made of snow glide using glide shoes (in der Gand and Zupancic,

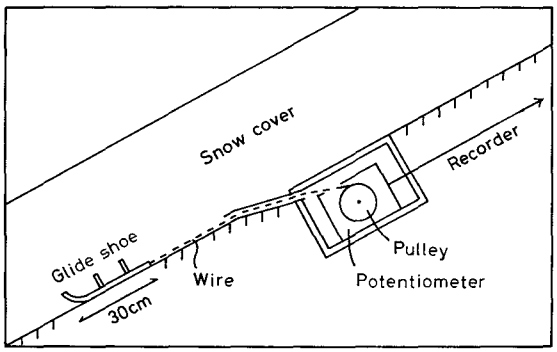

Fig. 1 Experimental arrangement for measuring snow glide.

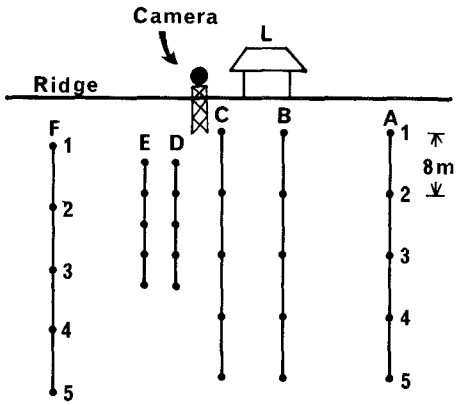

Fig. 2 Distribution of measuring points of snow glide on the south slope of avalanche observatory L, the Institute of Low Temperature Science.

1969). As shown in Fig. 1, the glide shoe is a kind of sled 0.30 m long and 0.15 m wide, on which two rectangular aluminum pieces 0.05 m high are rivetted to grip snow firmly. The glide shoes are placed on the slope before the first snowfall. After a snow cover has been built up on the shoe, the shoe will move with the glide of the snow cover. The movement of the shoe is transformed into the rotation of a potentiometer by means of a steel wire and is continuously recorded on a trip chart as a change in resistance of the potentiometer.

Spatial differences of snow glide will create a state of high stress in the snow cover, which will eventually lead to the formation of cracks and the start of avalanches. Hence, it is indispensable to know the spatial differences of snow glide, especially, along a line parallel to the fall line of the slope. Six such lines A to F, each with five measuring points numbered from 1 through 5, were aligned as shown in Fig. 2 over an area where avalanches had frequently occurred. Limited in number, however, glide shoes were not assigned to all measuring points.

In addition to the glide measurements, the area was photographed automatically every six hours to determine the time of occurrence of phenomena related to the snow glide.

II. 3 *Characteristics of snow glide on the slope covered with bamboo bushes*

Snow glide on the slope has been measured by Akitaya and Endo since the winter of 1973/74 (Akitaya, 1974 ; Endo and Akitaya, 1976). A typical result, obtained along line F in the winter of 1973/74, is given in Fig. 3 as the curves of glide distance against time. It is seen from the figure that each of upstream shoes F1 and F2 moved at nearly constant speed less than 0.01 m/day, while downstream shoes F4 and F5 increased each speed from 0.01 m/day at the initial stage to 0.10 m/day immediately before a crack was found between F3 and F4 on

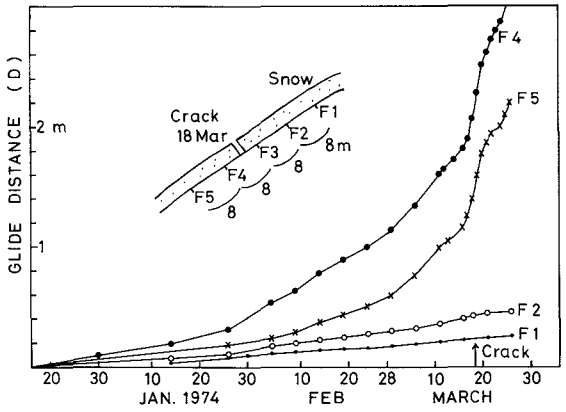

Fig. 3 Results of glide measurements along line F in the winter of 1973/74.

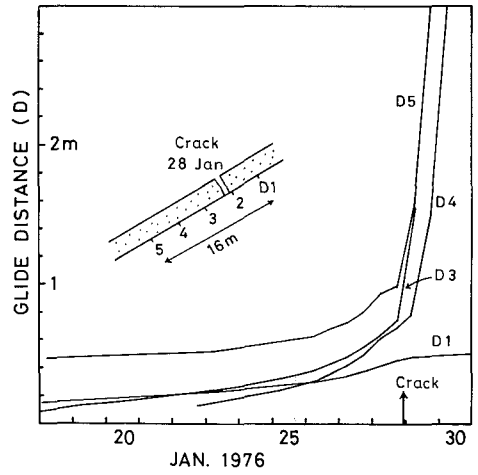

Fig. 4 Results of glide measurements along line D in the winter of 1975/76.

18 March 1974. Immediately after the crack formation, shoes F4 and F5, downstream the crack, intensely accelerated, while shoe F2, upstream the crack, decelerated.

Another result, obtained along line D in the winter of 1975/76, is shown in Fig. 4, where the same characteristics of glide as seen in Fig. 3 are again observed. That is, downstream shoes D3, D4 and D5 accelerated mildly before the crack formation and intensely after it. On the other hand, upstream shoe D1 moved at nearly constant speed until the crack formation and then somewhat decelerated.

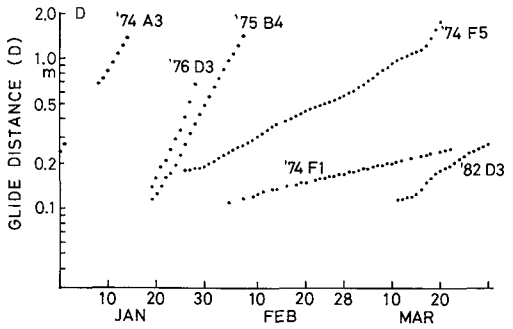

Fig. 5 Logarithmic plots of glide distance D against time t, omitting plots of $D<10$ cm.

A closer look at them shows that the accelerating glide of the downstream shoes began after they had glided some 10 to 20 cm, and that over 10 to 20 cm the glide distance increased exponentially with time as seen from Fig. 5.

II. 4 *Observations of the interface between snow and the ground*

The characteristic glide of snow mentioned in the previous section is undoubtedly due to the existence of bamboo bushes. In order to see their behavior, we made the vertical cross section of the snow cover at various stages of glide. Figure 6 is a photograph of the cross section along a contour line of the slope at an initial stage of snow glide. Though most of the bamboos lay down on the ground, some of them remained standing in the snow cover.

Fig. 6 Cross section of a snow cover cut vertically a contour line of a slope at an initial stage of snow glide.

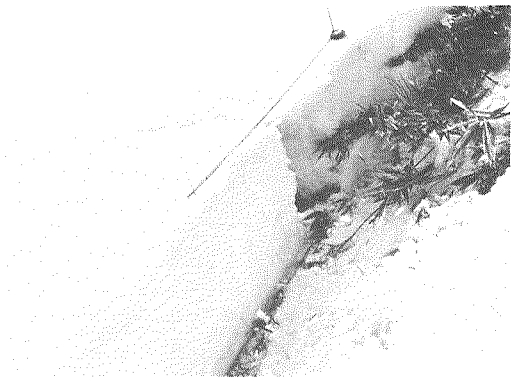

Fig. 8 Cross section of a snow cover cut vertically across a crack at the final stage of snow glide.

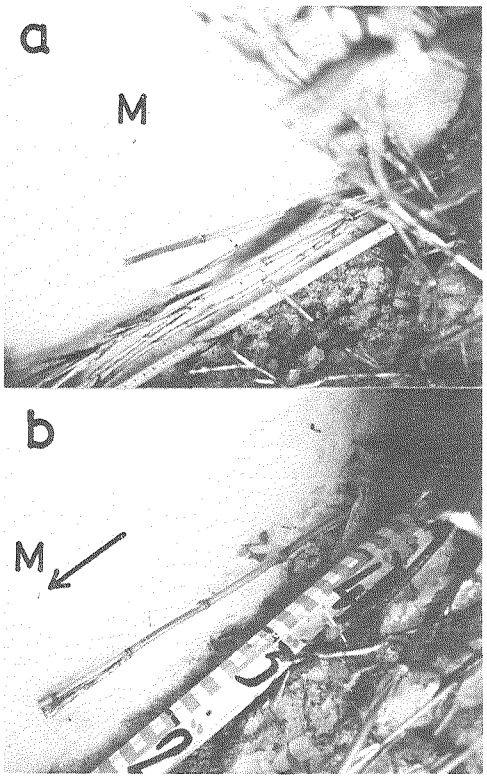

Fig. 7 A bamboo slipping out of a snow cover as snow glide proceeds, March 1977 (a : 15th ; b : 25th).
An arrow mark indicates the glide vector obtained from the movement of a marker M.

The standing bamboos changed their posture as the snow cover glided down the slope. Figures 7a and b are photographs taken on 15 and 25 March 1977, respectively, of the cross section along the fall line of the slope. An arrow mark in Fig. 7b is the glide vector for this 10-day interval obtained from the movement of a marker M. Comparing the two photographs, we can see that the standing bamboo in the snow cover had slipped out by the same length as the glide distance. If the glide distance of the snow cover was longer than the initial height of the standing bamboo, it would slip out completely and be pressed down under the snow cover.

The last presumption is confirmed by the photograph of the cross section along the fall line taken at the final stage of glide (Fig. 8). Downstream the crack, where the glide was sufficiently large, no bamboo was found in the snow cover, while upstream the crack there

remained a few standing bamboos in the snow cover.

II. 5 *Qualitative explanation of snow glide on the slope covered with bamboo bushes*

The behavior of bamboo bushes described in the previous section will give the following qualitative explanation of the characteristic glide of snow mentioned in Section II. 3 :

Fig. 9 A photograph of the observing area in early winter.

At the first heavy snowfall, most of bamboos fall down on the ground. But a few remain standing then are trapped in snow during the subsequent snowfalls. Covering the ground almost entirely, the fallen bamboos serve as a slippery base for the snow cover, whose glide is resisted effectively only by the standing bamboos. With progress in glide, the standing bamboos gradually slip out from the snow cover so that their resistance against the glide continues decreasing and the glide accelerates gradually. When the glide distance exceeds the initial height of the bamboos, all the bamboos slip out and, as a result, the glide accelerates strongly without any effective resistance.

The spatial differences of the glide may be attributed to those of the number of standing bamboos at the initial stage. The variance of this number is clear in a photograph of the observing area in early winter shown in Fig. 9, indicating an uneven distribution of bamboos which keep standing.

The formation of a crack is expected at the upstream boundary of a region in which the glide distance has exceeded the initial height of the bamboos. The expectation was, at least partly, confirmed by the observations compiled in Fig. 10, where the dotted arrow shows the fall line of the slope ; the solid line the position of a crack ; the open circle the position of a shoe ; and the numeral in parentheses a glide distance in centimeters immediately before the crack formation. In cases A, B, C and E, the glide distances upstream the crack were less than the height of bamboos (0.8 to 1.0 m) while those downstream the crack exceeded it. In cases D, F and G, the cracks may be considered to have originated at other places. In the latter two cases, the propagating cracks were stopped at the points where the stress was supposed to be little.

The arguments in this section are schematically summarized in Fig. 11, where thick solid lines show the bamboos orginally standing entrapped in the snow cover, their number densities being assumed higher in the upstream part than in the downstream part in the initial stage (I). Hence, at each successive stage, the glide distance must be longer in the downstream part than in the upstream part, as indicated by the arrows of varying length in

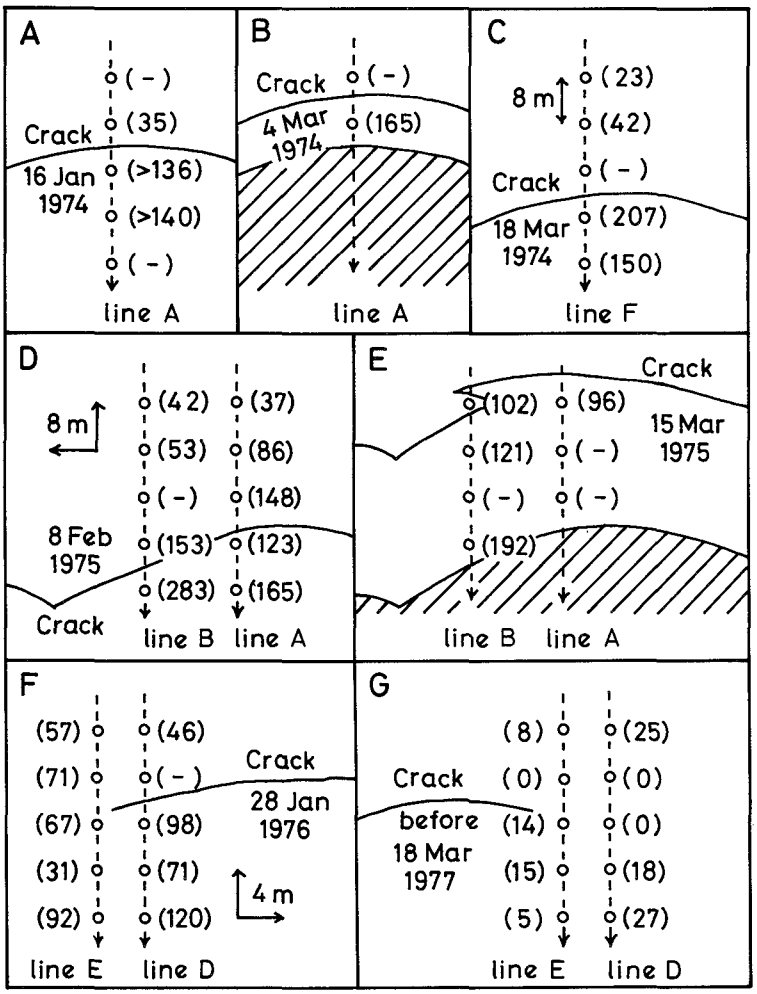

Fig. 10 Relation between the position of a crack and glide distance (cm) when it was formed.
The dotted arrow shows the fall line of the slope ; the solid line the position of a crack ; the open circle the position of a glide shoe ; and a numeral in parentheses a glide distance in centimeters immediately before the crack formation.

the figure. So, the length of the part of bamboo still left standing in snow becomes shorter in the downstream part (II). Eventually, all the bamboos fall down in the downstream part, while they are still standing in snow in the upstream part (III). Then, the intensively accelerated glide of the downstream part forms a high stress in the boundary and, consequently, a crack forms there (IV).

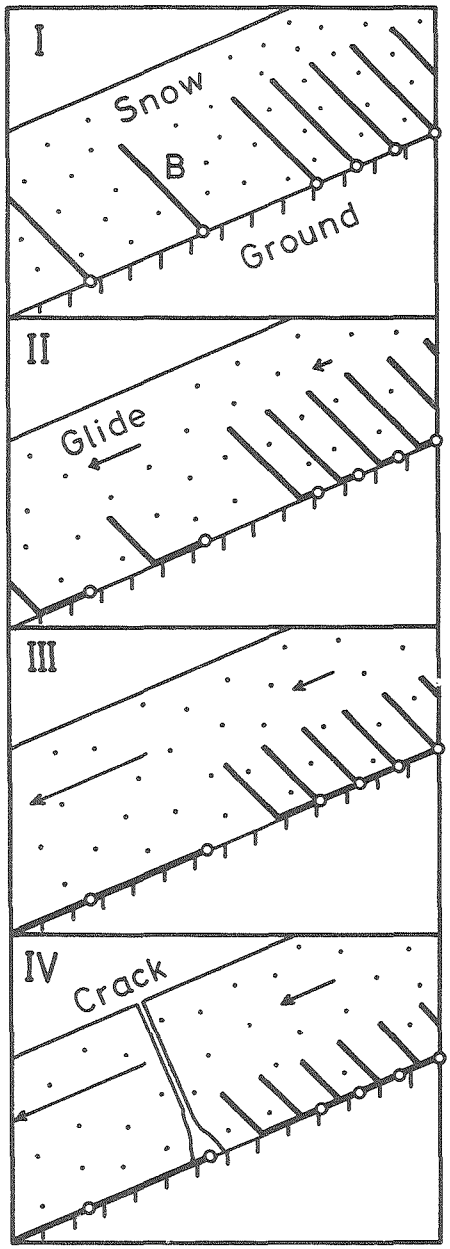

Fig. 11 Falling process of bamboos standing in a snow cover with progress in snow glide and crack formation. Thick solid lines B indicate bamboos originally standing entrapped in a snow cover.

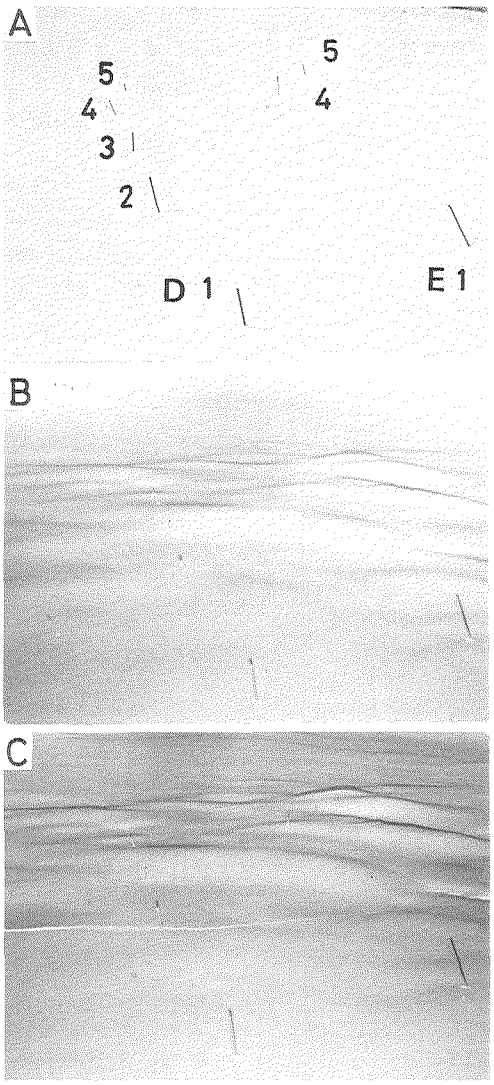

Fig. 12 Development of uncompressive snow undulations and formation of a crack.
Photographs were taken in January 1976 with the upside in the downstream direction----A on the 25th ; B and C on the 28th at 16 : 00 and 22 : 00, respectively.

II. 6 *Two kinds of snow undulations*

It has been long known that on a slope frequented by avalanches often appears snow undulation *after* the appearance of a crack and at a place far downstream of the crack.

Such an undulation has been considered to be a kind of folding of the snow cover caused by a compressive stress (Haefeli 1965). A compressive stress state can be realized at the downstream boundary of a region in which the glide distance is larger than in the surrounding regions, while a tensile stress state can be realized at the upstream boundary. As the tensile strength is usually smaller than the compressive strength of a snow cover, a crack at the upstream boundary is likely to appear before the appearance of a downstream undulation. Moreover, to create a compressive stress enough to cause an undulation, the mass of snow in the region per unit length of the downstream boundary must be sufficiently large, or in other words, the length of the region along the fall line must be long enough. Consequently the crack and the accompanied undulation must be far apart.

Now, photographs of the observed slope taken in January 1976 are shown in Figs. 12A, B and C. The first was taken on the 25th ; the second and third on the 28th at 16 : 00 and 22 : 00, respectively. Each pole, labeled in Fig. 12A, was to indicate the position of a glide shoe. As seen from their positions, the upside of the photographs is in the downstream direction. Snow undulation had appeared in Fig. 12B *before* a crack appeared just upstream of it in Fig. 12C. The undulation in Fig. 12, thus differing from the known ones in two essential characteristics, namely, the time of appearance relative to and the distance from the accompanied crack, is hardly considered to be caused by compression. For the sake of convenience, we will hereafter call such undulations as seen in Fig. 12 uncompressive, while the known ones compressive.

An uncompressive undulation is important because it may be used for predicting the formation of a crack and consequently the start of an avalanche. In fact, the undulation in Fig. 12 was already noticeable in the 27th ; the crack was formed on the 28th ; and an avalanche started at the crack on the 30th.

II. 7 *Formation mechanism of an uncompressive undulation*

In order to clarify the formation mechanism of uncompressive undulations, we studied the layer structure of them by making their cross sections along the fall line. One of the cross sections is illustrated in Fig. 13. It is disclosed that beneath a bump of the snow surface lies also a bump of ground and that the snow cover consists of two distinguishable layers, one forming a small heap covering the ground bump (layer I) and the other a continuous overlying layer (layer II). Also disclosed in layer II is a hollow trace A' of a small tree A, from which it follows that the whole snow cover glided about 1.5 m after formation of snow layer II. Now, on an assumption that the vertical compression of snow is insignificant, we can restore the original position of the surface of each layer by shifting

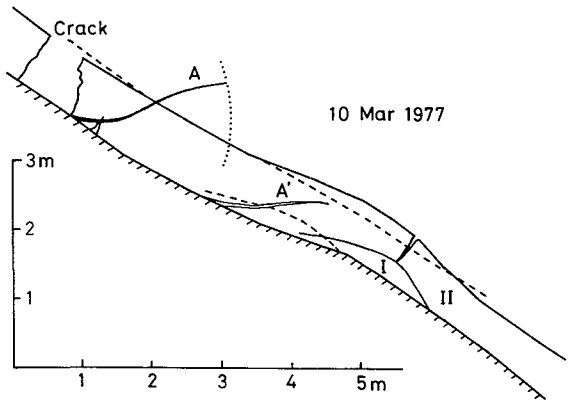

Fig. 13 Cross section of an uncompressive snow undulation along the fall line.
A' is the hollow trace of a small tree A left in the snow cover.

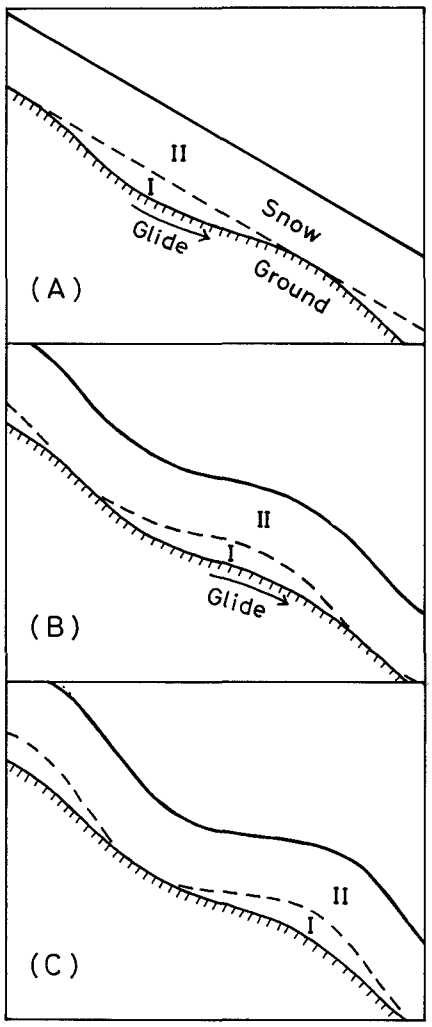

Fig. 14 Formation mechanism of uncompressive snow undulations by a glide process.

individual points of it by 1.5 m upstream. The broken lines in Fig. 13 represent the original surfaces thus restored, which shows that layer I accumulated in the upstream front of the ground bump and that layer II had a flat surface before the start of the glide. (The last two conclusions are valid even if the vertical compression of snow is not insignificant as long as it is homogeneous.)

Based on many such observations, we deduced a simple mechanism of the formation of an uncompressive undulation as schematically shown in Fig. 14. As a snowfall in a mountain region is usually accompanied by strong winds, the surface of a snow cover immediately after a snowfall is generally flat. In Fig. 14A, a light snowfall fills depressions of the ground, making layer I. Subsequent snowfalls (or one heavy snowfall) make layer II with a flat surface. As a depth enough to start the glide is attained, the whole snow cover begins to glide making an undulated surface as shown in Fig. 14B and eventually reaches the state shown in Fig. 14C, if snow has not fallen since the start of the glide. In the state shown in Fig. 14C, where the glide distance amounts exactly to a half of the wavelength of the ground undulation, the amplitude of the snow undulation will be twice that of the ground undulation.

III. Experimental computations of the resistance of bamboos against snow glide

We found in the previous chapter that, when a snow cover had been formed on a slope covered with bamboos, they either fell down on the ground or remained standing in the snow cover. These two groups of bamboos will resist the glide of snow in different ways. In order to describe the glide later quantitatively we will try in this chapter to find the resistance of each of the two groups as a function of glide speed and glide distance.

III. 1 *Resistance of the bamboos within a snow cover*

III. 1. 1 *Experimental procedures*

In order to study the resistance of the bamboos within a snow cover, we simulated in a cold room the motion of pulling out a bamboo from a snow mass in such a way that speed U of pulling it out, necessary force P and length D of its portion slipped out of snow will correspond, respectively, to glide speed, resistance and glide distance. The simulation arrangement is shown schematically in Fig. 15.

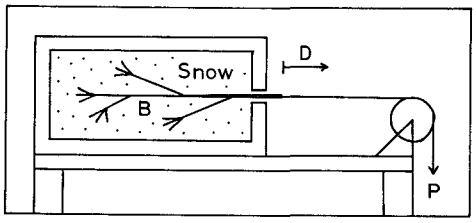

Fig. 15 Schematic diagram of a simulation apparatus for measuring resistance of a bamboo within a snow cover.

A specimen is prepared in a wooden box 0.90 m long, 0.45 m wide and 0.30 m deep with a hole in the center of a short side wall as follows : Natural snow stored in a cold room is gently pulverized and is deposited through a sieve in the box by half of its depth. Then, on the deposited snow is laid a bamboo about 0.9 m long with the part of its stem sticking out of the box through the hole, and pulverized snow is deposited again over th bamboo until it fills the box. After the specimen is kept at -5°C for one day, it is brought into a cold room maintained at a desired test temperature, 0°C, -1°C or -3°C ; measurements begin two days later to ensure that the whole specimen attains the test temperature. This temperature is chosen in accordance with the temperature of snow surrounding the actual standing bamboos, which ranges from 0°C to -3°C.

We measured either P for a constant U or D for a constant P, both as a function of time. In the former case, a traction device composed of a motor, a gear reducer and a worm-jack pulled the bamboo via a load cell, with which P was continuously measured. Meanwhile in the latter case, the constant force was supplied by a weight and D was measured intermittently with a rule graduated in mm. Since U is the time differential of D, we can obtain raw data concerning P, U and D by either method.

Now, in order to find a general relation among P, U and D from the raw data concerning them, it is convenient, or almost necessary, to have some guiding principle. Let S be the

contact area between the snow and the bamboo. Naturally, S is a decreasing function of D. The average horizontal component of a force acting on snow per unit area of the contact is given by P/S. As the snow will deform plastically at the contact point and as we treat either steady or slowly accelerating state, we may assume a simple equation

$$U=k\cdot(P/S)^m \tag{1}$$

where k and m are constants, depending on the temperature and the structure of snow.

III. 1. 2 *Dependence of S on D*

In a constant-speed experiment, S is proportional to P according to equation (1). Hence, the data of P against D for a constant U determine S as the function of D except a constant factor. Several constant-speed experiments were conducted at 0°C and −1°C with a speed ranging from 0.24 to 2.4 m/day. Three results are shown in Fig. 16. Except the initial stage of D which is less than about 10 cm, it is found that P, and hence S, is a decreasing function of D. Though the data are somewhat scattering, we may approximate S by

$$S=B\cdot\exp(-b\cdot D) \tag{2}$$

where B and b are constants. S must be zero for D larger than the length of the bamboo. Approximation (2) will give a discontinuity of S at value of D of the bamboo length. However, because of the values of b given in Fig. 16, the discontinuity is not so large that we may use the approximation for D up to the length of the bamboo.

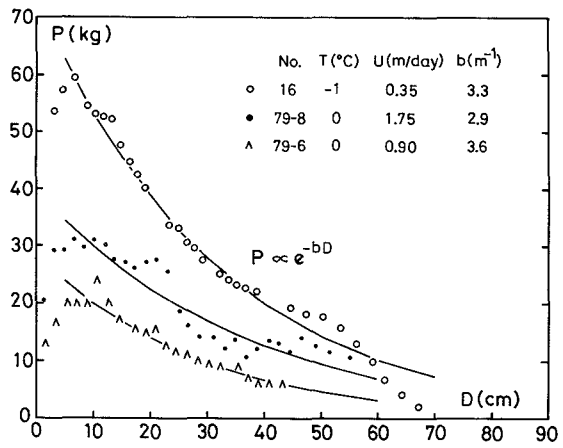

Fig. 16 Change in force P needed to pull out a bamboo against slipped-out length D in constant-speed experiments.

Using the approximation, we transform equation (1) into

$$U=A\cdot P^m\cdot\exp(m\cdot b\cdot D) \tag{3}$$

or

$$\log U=\log A+m\cdot\log P+m\cdot b\cdot D \tag{4}$$

where A is a constant.

III. 1. 3 *Determination of m, b and A*

Equation (4) shows that for constant P, $\log U$ is a linear function of D. Hence, in the plot of $\log U$ against D, the slope will give the value of $m\cdot b$, while the intersection of the

line of log U with the coordinate will give the value of ($\log A + m \cdot \log P$). Using the value of b such as shown in Fig. 16, we can indirectly determine the value of m and then the value of A from the data of a constant-force experiment. However, as the value of b may change from a specimen to another, we may rather determine the values of m, b and A of the same specimen.

Now, consider the case that we abruptly change the value of either U or P during a constant-speed or a constant-force experiment when $D = D_0$. Let U_1 and P_1 be the values of U and P just before and U_2 and P_2 those just after the change. Both the pair must satisfy equation (4) with the same values of A, m, b and $D = D_0$. Hence, we have

$$\log U_1 - \log U_2 = m \cdot (\log P_1 - \log P_2) \tag{5}$$

Equation (5) allows us to determine m independently.

As mentioned above, the values of A, m and b are better determined for one and the

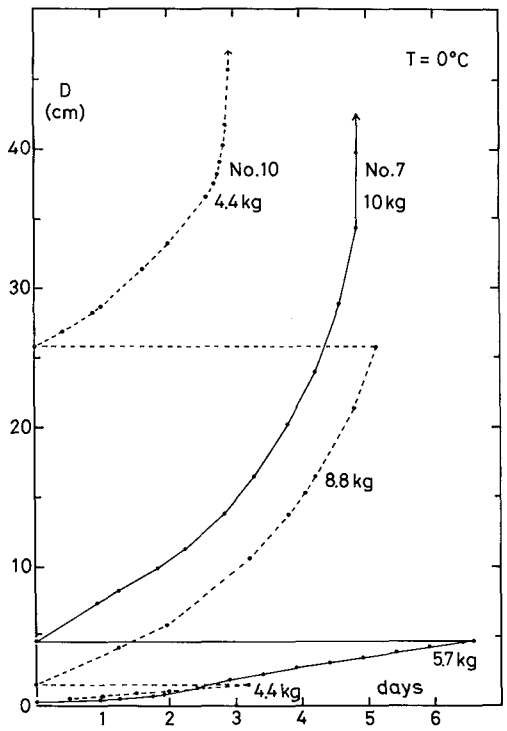

Fig. 17 Change in slipped-out length D of a bamboo against time t in constant-force experiments. Time is shifted to 0 each time the weight is changed during a constant-force experiment.

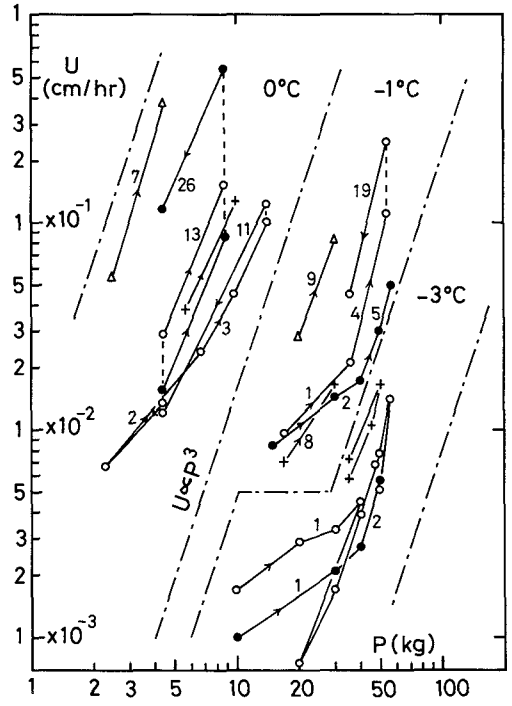

Fig. 18 Change in slipping-out speed U with the change of weight P.
A solid line with an arrow indicates the direction of the change.
Numerical figures with the unit of a centimeter along the solid line show the value of slipped-out length D at the change.

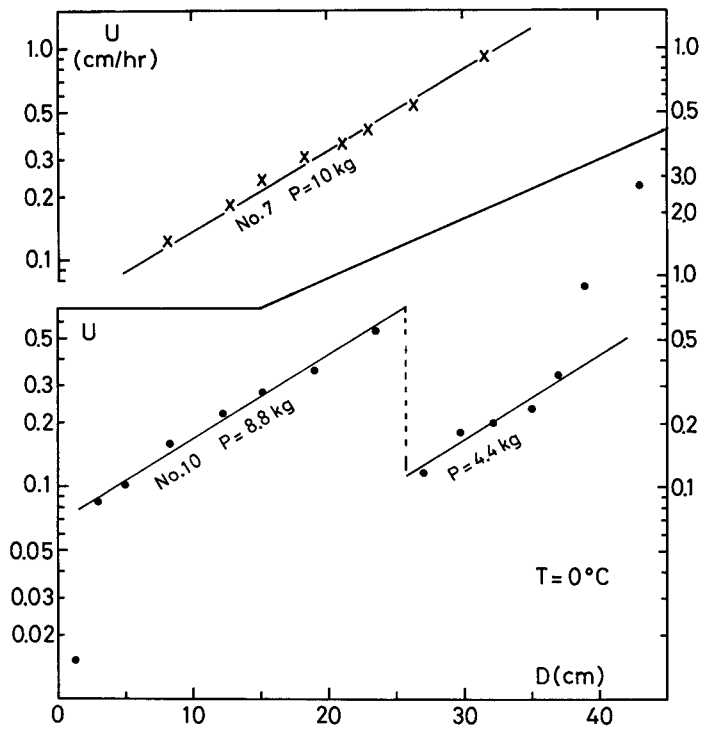

Fig. 19 Logarithmic plots of slipping-out speed U against slipped-out length D in constant-force experiments.

same specimen. So we changed the weight a few times during a constant-force experiment. Some results are shown in Fig. 17, where time is shifted to 0 each time the weight is changed so as to make the plot easy to read. It is seen from the figure that, though U is not a constant for a constant P, we can compute U_1 and U_2 from the plot in an enough accuracy to determine m. All of the data obtained by the change of the weight were compiled in Fig. 18, where two states, just before and after each change, are connected by a solid line with an arrow indicating the direction of the change. Numerical figures with the unit of a centimeter along the solid line show the value of D at the change. Evidently the slope of the solid line gives the value of m according to equation (5).

We can see from the figure that most of the changes gave a value of m of about 3 and that a few which gave a value of m of about 1 were all made at the initial stage of the experiment with the value of D less than a few centimeters. The resistance at such an initial stage may be insignificant practically. Hence, we may conclude that practically m is equal to 3.

By determining the value of m we can now compute the values of b and A from the plots of the values of U against the corrsponding values of D. From the raw data as shown in Fig.

Table 1 Values of b and A in the relation $U = A \cdot P^3 \cdot \exp(3b \cdot D)$

Exp. No.	b(m^{-1})	A($m \cdot kg^{-3} \cdot day^{-1}$)	T(°C)
79-6	3.6	3.6×10^{-5}	
79-8	2.9	2.9	
7	2.8	1.5	0 °C
9	1.7	3.6	
10	3.1	2.4	
〃	〃	2.9	
13	2.4	3.1×10^{-7}	
14	2.3	0.4	
15	2.9	0.9	−1 °C
〃	〃	0.4	
16	3.3	8.2	

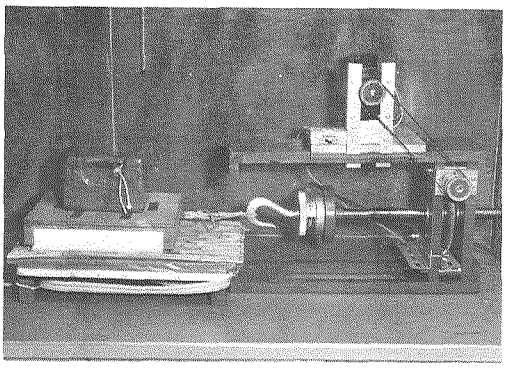

Fig. 20 Experimental apparatus for measuring resistance of fallen bamboos.

17, we made such plots, some of which are given in Fig. 19. Though somewhat scattered, the plots are well approximated by a straight line as expected from equation (4).

The values of b and A obtained from the experiments by the above mentioned method are listed in Table 1. As seen in the table, the values of b, ranging from 1,7 to 3.6 m^{-1} with a mean of 2.8 m^{-1}, seem to be independent of temperature, while those of A, being of the order of 10^{-5}m · kg^{-3} · day^{-1} at 0°C and around 10^{-7}m · kg^{-3} · day^{-1} at −1°C, are clearly dependent on it.

Though the values are somewhat scattered, we may approximate the relation among P, U and D by a simple analytical one given by equation (3) with $m=3$, $b=2.8$ m^{-1} and an appropriate value of A depending on temperature.

III. 2 *Resistance of the bamboos falling down on the ground*

In order to study the resistance of the fallen bamboos, we measured the force exerted on a snow block when it was pulled with a constant speed on an artificially simulated bamboo base, which was a sheet of plywood entirely covered with bamboos arranged parallel to the direction of the pull, as seen in Fig. 20.

The snow block is prepared by depositing pulverized snow in a wooden frame, 0.25 m long, 0.25 m wide and 0.05 m high, placed on the end of the base. The deposited snow is kept at −5°C for one day to allow enough sintering. Then, the frame is carefully replaced by a wooden cap 0.04 m deep, on which a weight is placed to simulate the weight of a natural snow cover. The cap is also utilized to pull the block. In the experiment, three weights are used to give a normal stress of 125, 215 and 375 kg/m^2 and the block is pulled with the traction device mentioned before with a constant speed U ranging from 0.01 to 4.00 m/day. The force is measured with a load cell and recorded continuously on a trip chart. The experiment was conducted in an environmental temperature of about +0.2°C to make the block wet.

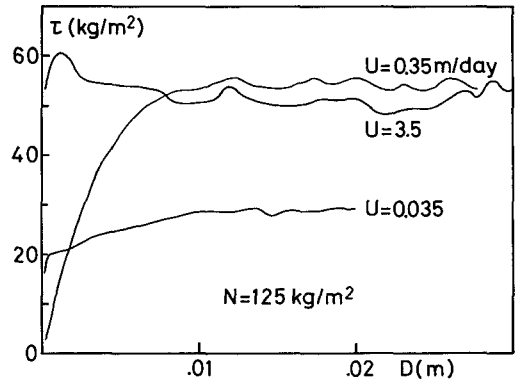

Fig. 21 Shear stress τ exerted by fallen bamboos versus glide distance D at various constant glide speeds U for normal stress N =125 kg/m².

Free water content at the bottom of the block was computed from occasional measurements of that of a dummy snow block.

Some results obtained for a normal stress N of 125 kg/m² are shown in Fig. 21 as the plot of shear stress τ (the measured force divided by the basal area of the block) against glide distance D. The figure shows that irrespective of glide speed U the shear stress settled down to a steady value after the block had glided 0.01 m or so. This steady value was considered the value of τ corresponding to the given values of U and N.

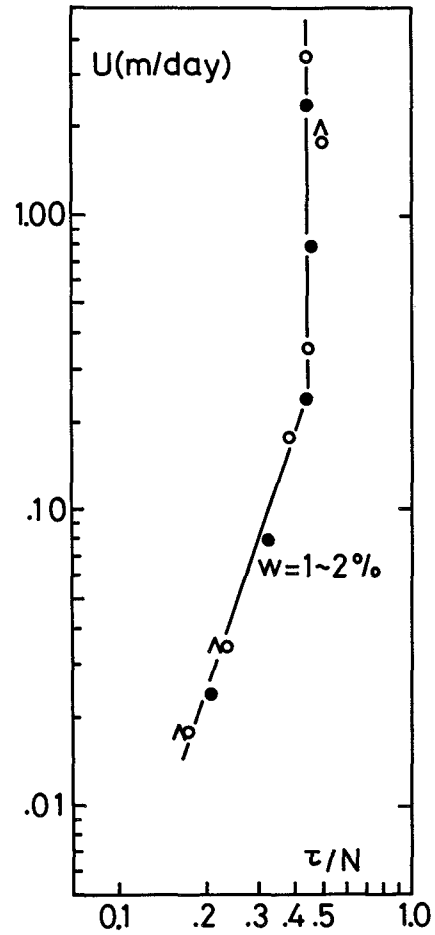

Fig. 22 Relation between glide speed U and friction coefficient τ/N of fallen bamboos.

As it was expected that τ/N, which is nothing but the friction coefficient, would depend on U, all obtained data are compiled in Fig. 22 as the plot of log U against log (τ/N). As expected, the figure shows the following relation between U and τ/N for the case of the free water content of 1 to 2 % :

$$\begin{aligned} \tau/N &= (U/B)^{1/3} \quad \text{for} \quad U \leq 0.45^3 \cdot B \\ \tau/N &= 0.45 \quad \text{for} \quad U > 0.45^3 \cdot B \end{aligned} \tag{6}$$

with the value B of about 2.4 m/day.

IV. Quantitative analysis of snow glide on a slope covered with bamboos

IV. 1 *Equations of snow glide*

The resistances of the two groups of bamboos having been represented by simple analytical forms, it is now possible to analyze the glide quantitatively. In this section we will derive the equations of snow glide for the most simple case of the glide of a uniform snow cover on a uniform slope, as illustrated in Fig. 23. Assume that the slope is entirely covered with fallen bamboos and that there remain n standing bamboos per unit area, each having length H. Now consider a snow block with a unit basal area and sides vertical to the slope. Because of the assumption of the uniform glide, the forces which are exerted on the block through the side walls cancel out ; and neglecting the inertia term, we have the equation of motion of the block of the following form as

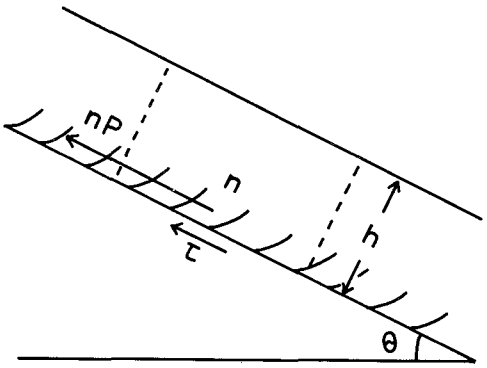

Fig. 23 Model of a snow cover on a slope covered with bamboo bushes.

$$h\cdot\rho\cdot\sin\theta = n\cdot P+\tau \tag{7}$$

where h is the thickness of the snow cover, ρ the density of snow, θ the inclination of the slope, P the resistance of one standing bamboo and τ the resistance of fallen bamboos. It follows from section III. 1. 3 that P is given as

$$\begin{aligned} &P=(U/A)^{1/3}\cdot\exp(-b\cdot D) && \text{for} \quad D<H \\ &P=0 && \text{for} \quad D\geq H \end{aligned} \tag{8}$$

where U is the glide speed and D the glide distance. The wet condition at the bottom of the snow cover being assumed, τ is given by equation (6) as

$$\begin{aligned} &\tau = h\cdot\rho\cdot\cos\theta\cdot(U/B)^{1/3} && \text{for} \quad U<0.45^3\cdot B \\ &\tau = 0.45\cdot h\cdot\rho\cdot\cos\theta && \text{for} \quad U\geq 0.45^3\cdot B \end{aligned} \tag{9}$$

where the factor $h\cdot\rho\cdot\cos\theta$ is the value of normal stress N.

Substituting equations (8) and (9) in equation (7), we have for $D<H$

$$U=A\cdot\left\{\frac{h\cdot\rho\cdot\sin\theta}{n\cdot\exp(-b\cdot D)+(A/B)^{1/3}\cdot h\cdot\rho\cdot\cos\theta}\right\}^3 \quad \text{for} \quad U<0.45^3\cdot B \tag{10 a}$$

$$U = A \cdot \left\{ \frac{h \cdot \rho \cdot (\sin\theta - 0.45 \cdot \cos\theta)}{n \cdot \exp(-b \cdot D)} \right\}^3 \qquad \text{for} \quad U \geq 0.45^3 \cdot B \qquad (10\,b)$$

and for $D \geq H$

$$U = B \cdot \tan^3\theta \qquad \text{for} \quad \theta \leq \arctan 0.45\ (=24.2^\circ) \qquad (11\,a)$$

$$\text{No steady state of } U \qquad \text{for} \quad \theta > \arctan 0.45\ (=24.2^\circ) \qquad (11\,b)$$

The region described by equation (10b) does not exist in the case that inclination θ is less than arctan 0.45, where the discontinuity of U at $D = H$, which appears when the regions (10a) and (11a) are connected, is due to the discontinuity of P in equation (8) and is practically negligible.

The last statement (11b) means that on a bamboo-covered slope steeper than 24.2° an avalanche starts when the snow cover has glided by a distance equal to the length of the bamboos. However, in the actual case it is unlikely that the whole snow cover glides by that distance and even if a part of the snow cover on a slope steeper than 24.2° has glided by that distance, it does not necessarily start as an avalanche because the surrounding part which has not yet glided enough may support it.

IV. 2 *Dependence of the glide on the density of the standing bamboos*

In this section we will investigate the effect of the density of the standing bamboos on the mode of glide by using the equations in the previous section.

As U is the time differential of D, equations (10a) and (10b) are integrated as follows :

$$t = \frac{1}{A \cdot (h \cdot \rho \cdot \sin\theta)^3} \int_0^D \{ n \cdot \exp(-b \cdot D) + (A/B)^{1/3} \cdot h \cdot \rho \cdot \cos\theta \}^3 \, dD \qquad \text{for} \quad 0 < D < D_c \qquad (12\,a)$$

and

$$t = t_c + \frac{1}{3 \cdot b \cdot A} \left\{ \frac{n}{h \cdot \rho \cdot (\sin\theta - 0.45 \cdot \cos\theta)} \right\}^3 \{ \exp(-3 \cdot b \cdot D_c) - \exp(-3 \cdot b \cdot D) \} \qquad \text{for} \quad D_c < D < H \qquad (12\,b)$$

where D_c is given only for $\theta > \arctan 0.45$ by

$$D_c = \frac{1}{b} \cdot \ln \left\{ \frac{0.45 \cdot n \cdot (B/A)^{1/3}}{h \cdot \rho \cdot (\sin\theta - 0.45 \cdot \cos\theta)} \right\} \qquad (13)$$

and t_c is the time when D reaches D_c. It must be noted here that the value of D_c may exceed H. In that case, and also in the case that θ is not larger than arctan 0.45, the part described by equation (12b) does not exist and D_c in equation (12a) must read as H.

Now, in order to examine the effect of the density of standing bamboos, we numerically calculated the dependence of D on t from equations (12a) and (12b) for various values of n, where for comparison with the result of field observations we used the following values,

which are thought to be representative of the field conditions described before :

$H=1$ m (Height of the standing bamboos)
$h=1$ m (Depth of the snow cover)
$\rho=300$ kg/m^3 (Mean density of the snow cover)
$\theta=30°$ (Inclination of the slope)
$b=2.8$ m^{-1} (Mean of experimental values in Table 1)
$B=2.4$ m·day^{-1} (Experimental value at 0°C)
$A=10^{-7}$m·kg^{-3}·day^{-1} (Order of experimental values at -1℃ in Table 1).

The results are shown in Fig. 24, where the vertical lines for $D \geq 1$ m correspond to the statement (11b), as in this case the inclination of the slope is larger than 24.2°.

The figure clearly shows that the spatial differences of the snow glide shown in Figs. 3 and 4 are caused by the density of standing bamboos. According to the calculation, a region of the snow cover containing more than 5 standing bamboos per square meter cannot reach the unstable state (D larger than H) for more than 3 months, namely, throughout the winter. This is in accord with the observation that n was usually larger than 5 in a stable snow cover upstream of a crack.

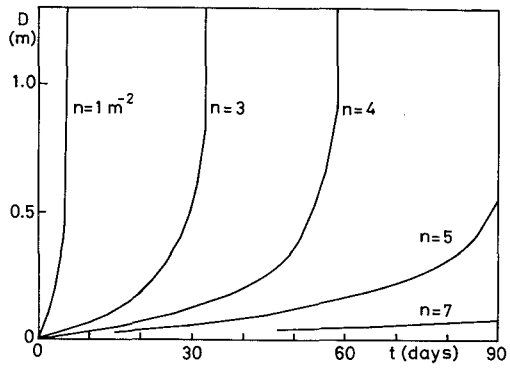

Fig. 24 Calculated curves of glide distance D against time t for various densities n of standing bamboos in the snow cover.

V. Distributions of stress and glide speed in the snow cover

As pointed out before, spatial differences of glide in a snow cover create a stressed state in it ; and as a result the snow cover will fracture at a point when the stress there reaches a critical value. Also, field observations showed that a crack is usually formed near the upstream boundary of a region of the snow cover after the region has glided enough to prostrate all the bamboos initially contained in it. In this chapter we will determine the distributions of stress and glide speed in this region and compute the critical stress. Then we will compare the computed value with the values of tensile strength of snow obtained by other researchers.

V. 1 *Model and equations*

We consider a snow cover with uniform thickness h gliding slowly on a slope of uniform inclination θ, whose surface is "smooth" between upstream point O and downstream point L and "rough" elsewhere as shown in the upper part of Fig. 25. The "smooth" surface means

the surface on which all the bamboos remain prostrated on the ground and hence the resistance against snow glide exerted by the surface is only the shear stress τ given by equation (6), while the "rough" surface means the surface on which some of the bamboos remain entrapped in a snow cover giving an additional resistance against snow glide.

We naturally expect that near a boundary of the smooth and the rough surface, the glide speed of snow is lower on the rough surface than on the smooth surface. The speed must be continuous at the boundary before the formation of a crack ; so, in the smooth region shown in Fig. 25 the speed increases foward downstream near point O creating a tensile state while it increases foward upstream near point L creating a compressive state. As the stress is continuous in snow, there must be a point denoted by L_0 where the longitudinal stress in snow becomes zero between points O and L. The portion of the snow cover between points O and L_0 is called to be in a tensile zone and that between L_0 and L to be in a compressive zone.

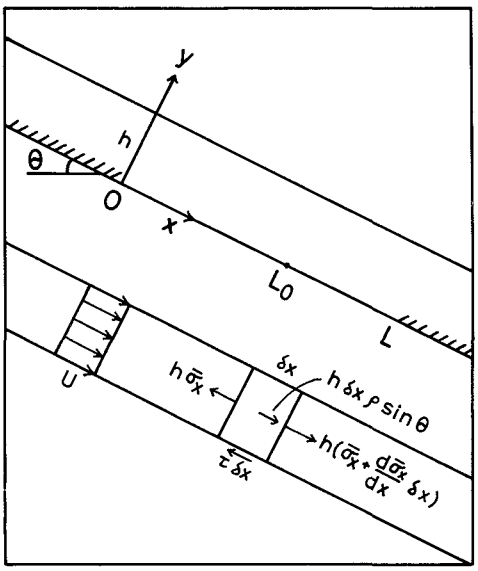

Fig. 25 Slope geometry prior to formation of a crack and coordinate reference.

We take point O as the origin, the x-axis along the slope, positive downstream ; the y-axis perpendicular to the slope, positive upward ; and the z-axis perpendicular to the plane of the paper. Now, consider a column of snow parallel to the y-axis with a base of a small length δx along the x-axis and of a unit length along the z-axis. Neglecting the inertia term, we have the following equation of motion of the column :

$$h\cdot(\mathrm{d}\bar{\sigma}_x/\mathrm{d}x)-\tau+h\cdot\rho\cdot\sin\theta=0 \tag{14}$$

where τ is the shear stress on the surface of the slope given by equation (6), ρ is the density of snow and $\bar{\sigma}_x$ is the mean over the snow depth of normal stress σ_x on the $y\cdot z$-plane :

$$\bar{\sigma}_x = h^{-1}\int_0^h \sigma_x \mathrm{d}y \tag{15}$$

It has been known that, at a low stress, homogeneous snow exhibits the linear viscous behavior governed by the following equations (Haefeli, 1939 ; Shinojima, 1967) :

$$\dot{\varepsilon}_x = +(1/\eta_x)\sigma_x-(\nu_y/\eta_y)\sigma_y-(\nu_z/\eta_z)\sigma_z \tag{16a}$$

$$\dot{\varepsilon}_y = -(\nu_x/\eta_x)\sigma_x+(1/\eta_y)\sigma_y-(\nu_z/\eta_z)\sigma_z \tag{16b}$$

$$\dot{\varepsilon}_z = -(\nu_x/\eta_x)\,\sigma_x - (\nu_y/\eta_y)\,\sigma_y + (1/\eta_z)\,\sigma_z \tag{16c}$$

where $(\dot{\varepsilon}_x, \dot{\varepsilon}_y, \dot{\varepsilon}_z)$ and $(\sigma_x, \sigma_y, \sigma_z)$ are the principal components of the strain-rate and those of the stress tensor, respectively, (here the coordinate system is so taken that its x-, y- and z-axis coincide with the respective principal axes of the tensor), and ν_λ and η_λ $(\lambda = x, y, z)$ are both the two value functions, which are ν_e and η_e when σ_λ is positive (tensile) and are ν_c and η_c when σ_λ is negative (compressive). The four values are all nonnegative. Particularly

$$\nu_e \simeq 1/2,\ \nu_c \simeq 0 \tag{17}$$

according to Shinojima (1967).

Now, we assume the principal axes of the stress tensor coincide with our x-, y- and z-axis defined earlier. Then σ_y is compressive everywhere and hence ν_y is zero. As there is no strain in the z-direction, $\dot{\varepsilon}_z$ is also zero. So, it follows from equation (16c) that σ_x and σ_z are of the same sence ; that is, both are tensile or both are compressive. Hence, from equations (16a, b, c), we have in the tensile zone

$$\sigma_x = (4/3)\cdot\eta_e\cdot\dot{\varepsilon}_x\ ;\ \sigma_y = \eta_c\cdot(\dot{\varepsilon}_x + \dot{\varepsilon}_y)\ ;\ \sigma_z = (1/2)\cdot\sigma_x \tag{18}$$

and in the compressive zone

$$\sigma_x = \eta_c\cdot\dot{\varepsilon}_x\ ;\quad \sigma_y = \eta_c\cdot\dot{\varepsilon}_y\ ;\quad \sigma_z = 0 \tag{19}$$

Now, we assume that the snow cover mostly moves at the bottom, so that the x component of velocity is almost independent of y. Then, $\dot{\varepsilon}_x$ is nearly equal to $\mathrm{d}U/\mathrm{d}x$, where U is the glide speed ; and hence, independent of y. Thus, we have

$$\bar{\sigma}_x = (4/3)\cdot\eta_e\cdot(\mathrm{d}U/\mathrm{d}x) \quad \text{in the tensile zone} \tag{20}$$

and

$$\bar{\sigma}_x = \eta_c\cdot(\mathrm{d}U/\mathrm{d}x) \quad \text{in the compressive zone} \tag{21}$$

from these equations and equation (14), we have

$$(4/3)\,h\cdot\eta_e\cdot(\mathrm{d}^2U/\mathrm{d}x^2) - \tau(U) + h\cdot\rho\cdot\sin\theta = 0 \tag{22}$$

and

$$h\cdot\eta_c\cdot(\mathrm{d}^2U/\mathrm{d}x^2) - \tau(U) + h\cdot\rho\cdot\sin\theta = 0 \tag{23}$$

respectively, in the tensile zone and the compressive zone.

V. 2 *Approximate solution of U in an analytical form*

As $\tau(U)$ is given explicitly by equation (6), equation (22) or (23) can be solved numerically when the values of the constants and the boundary conditions are given. But, in order to

study general tendencies of U, we will try to have an analytical form of U even if approximately. Now, curve A in Fig. 26 is the plot of τ/N by equation (6), while broken line B is the plot of

$$(\tau/N)=\mu+\lambda\cdot U\ ;\quad \mu=0.2 \text{ and } \lambda=1.0 \text{ day/m} \tag{24}$$

It is seen from Fig. 26 that for U less than 0.3 m/day curve A is well approximated by linear function (24). As a crack was always found in our obsevations when a glide speed was less than 0.3 m/day, we use expression (24) with $h\cdot\rho\cdot\cos\theta$ as the value of N in solving equations (22) and (23), which are now written respectively as

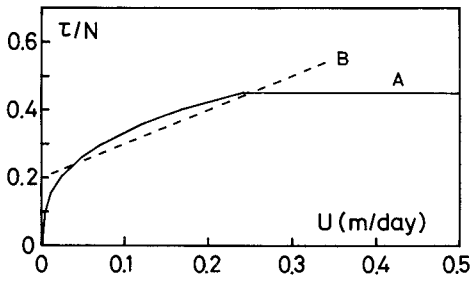

Fig. 26 Relation between friction coefficient τ/N of fallen bamboos and glide speed U. Curve A is the relation given by equation (6); curve B is an approximation to curve A.

$$\mathrm{d}^2U/\mathrm{d}x^2-N_t^2\cdot U+q_t=0 \qquad (\text{for } 0\le x\le L_0) \tag{25}$$

where

$$N_t^2=\frac{3\cdot\lambda\cdot\rho}{4\cdot\eta_e}\cos\theta \quad\text{and}\quad q_t=\frac{3\cdot\rho}{4\cdot\eta_e}(\sin\theta-\mu\cdot\cos\theta)$$

and

$$\mathrm{d}^2U/\mathrm{d}x^2-N_c^2\cdot U+q_c=0 \quad (\text{for } L_0\le x\le L) \tag{26}$$

where

$$N_c^2=\frac{\lambda\cdot\rho}{\eta_c}\cos\theta \quad\text{and}\quad q_c=\frac{\rho}{\eta_c}(\sin\theta-\mu\cdot\cos\theta)$$

The solution of equation (25) with the boundary conditions $U=U_o$ at $x=0$ and $\mathrm{d}U/\mathrm{d}x=0$ at $x=L_o$ is given by

$$U=K-(K-U_0)\frac{\cosh\{N_t\cdot(L_0-x)\}}{\cosh(N_t\cdot L_0)} \tag{27}$$

while that of equation (26) with the boundary conditions $U=U_L$ at $x=L$ and $\mathrm{d}U/\mathrm{d}x=0$ at $x=L_o$ is given by

$$U=K-(K-U_L)\frac{\cosh\{N_c\cdot(x-L_0)\}}{\cosh\{N_c\cdot(L-L_0)\}} \tag{28}$$

where K is defined by

$$K=\frac{q_t}{N_t^2}=\frac{\sin\theta-\mu\cdot\cos\theta}{\lambda\cdot\cos\theta}=\frac{q_c}{N_c^2} \tag{29}$$

The value of U at $x=L_o$ of equation (27) must be the same as that of equation (28). Hence, we have the following equation

$$(K-U_0)\cdot\cosh\{N_c\cdot(L-L_0)\}=(K-U_L)\cdot\cosh(N_t\cdot L_0) \tag{30}$$

Because of equation (30), of four quantities U_0, U_L, L_0 and L only three are independent.

Now, from the distributions of glide speed, equations (27) and (28), the distributions of stress in the tensile and the compressive zone are obtained as

$$\bar{\sigma}_x=\frac{4}{3}\cdot\eta_e\cdot N_t\cdot(K-U_0)\cdot\frac{\sinh\{N_t\cdot(L_0-x)\}}{\cosh(N_t\cdot L_0)} \tag{31}$$

and

$$\bar{\sigma}_x=-\eta_c\cdot N_c\cdot(K-U_L)\cdot\frac{\sinh\{N_c\cdot(x-L_0)\}}{\cosh\{N_c\cdot(L-L_0)\}} \tag{32}$$

The maximum tensile stress is naturally found at $x=0$, while the maximum compressive stress at $x=L$. Their values are obtained from the distributions given by equations (31) and (32) as

$$\bar{\sigma}_x(0)=(4/3)\cdot\eta_e\cdot N_t\cdot(K-U_0)\cdot\tanh(N_t\cdot L_0) \tag{33}$$

and

$$\bar{\sigma}_x(L)=-\eta_c\cdot N_c\cdot(K-U_L)\cdot\tanh\{N_c\cdot(L-L_0)\} \tag{34}$$

Some interesting conclusions are obtained from equations (30), (33) and (34). Assume that $U_0=U_L$. Then from equation (30) we have

$$\frac{\text{The length of the tensile zone}}{\text{That of the comprressive zone}}=\frac{L_0}{L-L_0}=\frac{N_c}{N_t}=\left(\frac{4\cdot\eta_e}{3\cdot\eta_c}\right)^{\frac{1}{2}}$$

and then from equations (33) and (34)

$$\frac{\text{Maximum tensile stress}}{\text{Maximum compressive stress}}=\frac{\bar{\sigma}_x(0)}{\bar{\sigma}_x(L)}=-\left(\frac{4\cdot\eta_e}{3\cdot\eta_c}\right)^{\frac{1}{2}}$$

According to Shinojima (1967), η_c is two-thirds the value of η_e. Then, the above ratio becomes $\sqrt{2}$. Now the condition $U_0=U_L$ may mean that the upstream rough surface and the downstream rough surface are in similar conditions. In this case the absolute value of maximum tensile stress is $\sqrt{2}$ times that of maximum compressive stress. This may be another reason for the formation of a crack before the appearance of compressive undulation mentioned in Chapter II.

V. 3 *Numerial computation of the distributions and comparison with observed values*

The main purposes of this section are to compute the distributions of glide speed and stress in an actual snow cover immediately before the formation of a crack and to compare the maximum tensile stress thus obtained with the values of tensile strength of snow obtained by other researchers. Throughout the section, the following values will be used to specify snow :

$\rho = 300$ kg/m^3 ;

$\eta_e = 21000$ kg·day/m^2 ; $\eta_c = 14000$ kg·day/m^2

(obtained by Shinojima (1967) for snow of 300 kg/m^3 at -5°C) ;

$\mu = 0.20$; $\lambda = 1.00$ day/m.

Now, for determining the distributions in a snow cover on a "smooth" slope, it is necessary to specify three of the four quantities, U_0, U_L, L_0 and L. However, there are few measurements of U_L and L of an actual snow cover. Fortunately, however, the distributions in the tensile zone can be determined by specifying only U_0 and L_0. In order to estimate their values immediately before the formation of a crack, the results of glide measurements such as shown earlier in Figs. 3 and 4 are rearranged in Fig. 27, where the abscissa represents the distance along the slope with each number showing the position of an individual glide shoe and the ordinate the glide speed determined from the glide distance for one day. The arrows show the position at which a crack was formed. Each number along the plots shows the number of days counted reversely from the date of crack formation. Namely, 1 means that the speed is computed from the glide distance for 24 hours just before the crack formation.

According to the figure, the glide speed just upsteam of the crack immediately before the formation of the crack, regarded as U_0, ranged from 0.05 to 0.12 m/day, while the maximum glide speed, regarded as $U(L_0)$, ranging from 0.12 to 0.20 m/day, appeared about 10 m downstream of the crack.

In order to compare with these values obtained from observations, we now calculate the distribution of speed by equation (27) and that of stress by equation (31) for $\theta = 30°$, $U_0 = 0.08$ m/day and $L_0 = 10$ m. The result is shown in Fig. 28, where the distributions for $\theta = 30°$, $U_0 = 0$ m/day and $L_0 = 10$ m are also given. The maximun speed $U(L_0)$ of about 0.18 m/day for $U_0 = 0.08$ m/day is close to the value obtained from observations.

On the other hand, the maximum tensile stress is only 600 kg/m^2 for $U_0 = 0.08$ m/day and 750 kg/m^2 even for $U_0 = 0$ m/day, both of which are very small in comparison with the tensile strength, 3000 to 10000 kg/m^2, of snow of a density of 300 kg/m^3 reported by others (Keeler and Weeks, 1963 ; Watanabe, 1977). The reason for the discrepancy may be that our computed stress is rather a mean over the snow depth at $x = 0$, $\bar{\sigma}_x$ (0), and is not the stress at the point of crack formation where a high stress concentration is expected. Hence, our computed values of stress must be compared with the values obtained from the experiments simulating our specified condition.

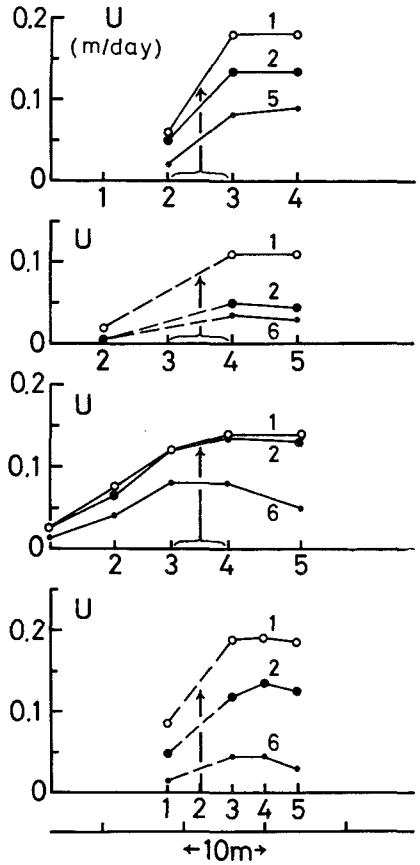

Fig. 27 Distribution of glide speed U along the slope measured before the formation of a crack. The abscissa represents the distance along the slope with the number showing the position of a glide shoe. The arrows show the position of a crack formed. The number along the plots shows the number of days counted reversely from the date of crack fromation.

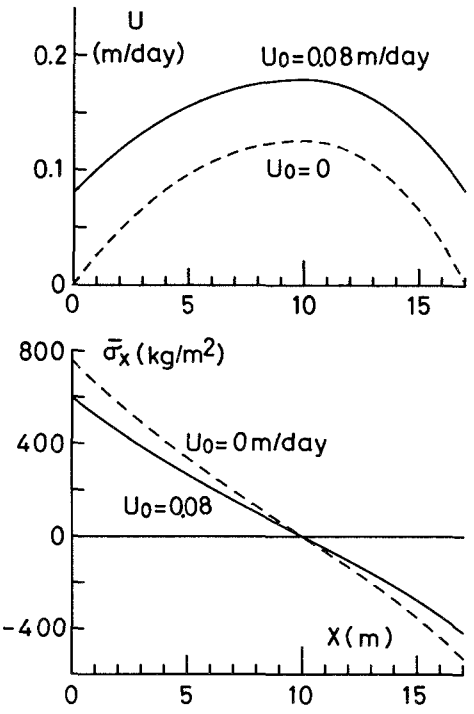

Fig. 28 Distributions of glide speed and stress calculated by equations (27) and (31) for $\theta=30°$, $L_0=10$ m and $U_0=0$ and 0.08 m/day.

McClung (1979) carried out a fracture experiment of snow. He allowed natural falling snow particles to deposit on a large table 0.9 m wide and 1.8 m long, a part of whose surface was smooth. After the depth of deposited snow had amounted to about 0.3 m, he tilted the table until the snow fractured. He deduced the tensile strength from the angle of tilt. Narita (1982) also conducted a similar experiment. Their results are plotted in Fig. 29. For a snow of a density of 300 kg/m^3, their values ranged from 300 to 1200 kg/m^2 with a mean of about 750 kg/m^2, which agreed to our results. We may consider reasonable that a value of maximum stress, say, 750 kg/m^2, serves as a measure of an alarm for the formation of a crack.

Now, for given snow specifications and slope angle, the maximum stress is determined by U_0 and L_0. However, both the variables are hard to measure. So we will seek another variable. From equation (27), the maximum glide speed $U(L_0)$ is given as

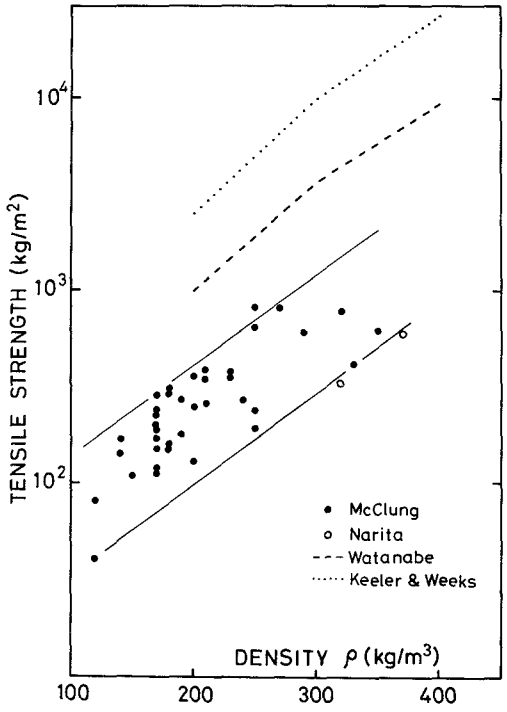

Fig. 29 Tensile strength of snow versus snow density.

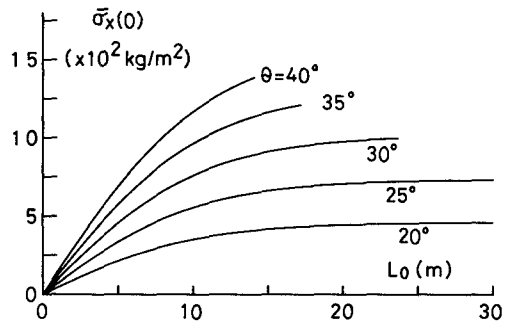

Fig. 30 Relation between maximum tensile stress $\bar{\sigma}_x(0)$ on a slope and length L_o of tensile zone for slope angles of 20°, 25°, 30°, 35° and 40°.

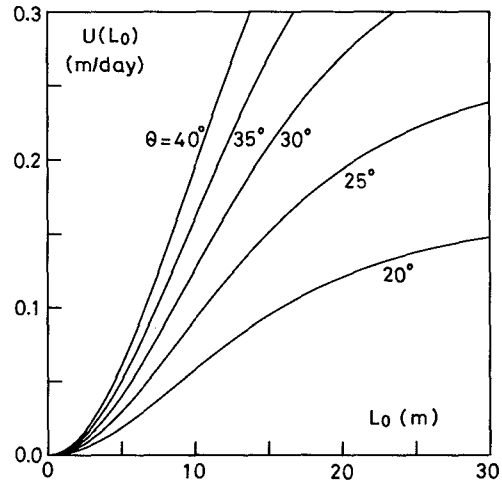

Fig. 31 Relation between maximum glide speed $U(L_o)$ on a slope and length L_o of tensile zone for slope angles of 20°, 25°, 30°, 35° and 40°.

$$U(L_0)=K-(K-U_0)/\cosh(N_t\cdot L_0) \tag{35}$$

which is again determined by U_0 and L_0. Hence, for a given U_0, the maximum stress is determined only by $U(L_0)$. We will denote the maximum speed $U(L_0)$ which gives the maximum stress of 750 kg/cm² by U_S. It is expected from a comparison between equations (33) and (35) that U_S is an increasing function of U_0. Hence, the value of U_S for $U_0=0$ is the minimum value of glide speed necessary (not necessarily sufficient) to cause the stress of 750 kg/m² somewhere. We will call this value of U_S for $U_0=0$ the critical speed and denote it by U_{cr}.

The value of U_{cr} is obtained using Figs. 30 and 31, which give the plots of equations (33) and (35), respectively, for the snow specified at the beginning of this section and for the slope

angles of 20°, 25°, 30°, 35° and 40° with $U_0=0$. We first find L_0 corresponding to $\bar{\sigma}_x$ *(0)* of 750 kg/m^2 in Fig. 30 and then find U_{cr} as the value of $U(L_0)$ corresponding to L_0 in Fig. 31.

VI. Concluding remarks

The present author has met with some success in his effort to give a unified quantitative description of the behavior of a snow cover on a slope covered with bamboo bushes. Particularly, as a result, it is now possible to predict the formation of a crack in the snow cover from data on glide speed or glide destance or both, if the density, temperature, and viscous coefficients (η_e, ν_e) of snow and the inclination of the slope are given.

As for vegetation growing on a slope, this study has dealt only with bamboo bushes, but the same reasoning can naturally be applied to tall grasses, which are common in other districts of Japan than Hokkaido. If the resistance of the grasses kept standing in snow and that of the grasses which fell down under snow are experimentally determined, the behavior of a snow cover on such a slope can also be described quantitatively.

The glide of a snow cover is not the sole cause of the instability of a snow mass at the bottom of it. As has been accepted by many researchers, an increase in free water content in snow is surely one of the main causes of the instability during the snow-melting season. Many problems remain to be solved concerning factors which give rise to the instability.

Acknowledgements

The author would like to express his gratitude to Professors T. Huzioka, Y. Suzuki and G. Wakahama and Drs. H. Simizu, K. Fujino and E. Akitaya, all of the Institute of Low Temperature Science, for their encouragement and valuable advice in this work. He is also indebted to Dr. S. Takikawa for his kindness to offer logistic support to the field work at Toikanbetsu.

References

Akitaya, E. 1974 Studies of the behavior of snow cover on slope III. —glide motion of snow. *Low Temp. Sci., Ser.* **A32,** 97-104.

Akitaya, E. 1975 Studies of the behavior of snow cover on slope V. —glide motion of snow and formation of crack. *Low Temp. Sci., Ser.* **A33,** 103-108.

Endo, Y. and Akitaya, E. 1976 Studies of the behavior of snow cover on mountain slope VI. — formation and mechanism of bump-shaped undulation. *Low Temp. Sci., Ser.* **A34,** 99-110.

Endo, Y. and Akitaya, E. 1977 Glide mechanism of a snow cover on a slope covered with bamboo bushes. *Low Temp. Sci., Ser.* **A35,** 91-104.

Endo, Y. and Akitaya, E. 1978 Glide mechanism of a snow cover on a slope covered with dwarf bamboo bushes. *In* Deuxieme Rencontre Internationale sur la Neige et les Avalanches,

1978, Grenoble, France. ANENA 71-80.
Endo, Y. 1980 Glide mechanism of a snow cover on a slope covered with bamboo bushes II. *Low Temp. Sci., Ser.* **A39,** 81-89.
Haefeli, R. et al. 1939 Der Schnee und seine Metamorphose. *Beitr. Geol. Schweiz-Geotechn. Ser. Hydrologie, Lieferung* **3,** 69-241.
Haefeli, R. 1963 Stress transformations, tensile strengths and rupture processes of the snow cover. *In* Ice and Snow. M. I. T. Press, Cambridge, Mass., 560-575.
in der Gand, H. R. and Zupancic, M. 1966 Snow gliding and avalanches. *IUGG, Intern. Assoc. Sci. Hydrol.,* Publ. 69, 230-242.
Japanese Society of Snow and Ice 1964 The classification of avalanche. *Seppyo* **26,** 195-198.
Keeler, C. M. and Weeks, W. F. 1968 Investigations into the mechanical properties of alpine snow-packs. *J. Glaciol,.* **7,** 253-271.
McClung, D. M. 1975 Creep and the snow-earth interface condition in the seasonal alpine snow-pack. *In* Snow Mechanics, Proc. of the Grindelwald Symp., April 1974. IAHS-AISH Publ. No. 114, 236-248.
McClung, D. M. 1979 In-situ estimates of the tensile strength of snow utilizing large sample sizes. *J. Glaciol.* **22,** 321-329.
Mellor, M. 1968 Avalanches. Report No. III-**A3d**, CRREL.
Narita, H. 1983 An experimental study on tensile fracture of snow *Contri. Inst. Low Temp.* (in press).
Shinojima, K. 1967 Study on the visco-elastic deformation of deposited snow. *In* Physics of Snow and Ice, part 2 (H. Oura, ed.), Inst. Low Temp. Sci., Sapporo, 875-907.
U. S. Forest Service, Department of Agriculture 1961 Snow avalanches —a handbook of fore-casting and control measures. *Agriculture handbook* No. **194,** 1-84.
Watanabe, Z. To be published.
Yamada, Y. 1977 On a new method for snow gliding measurement —gear-type glide-meter—. *The Report of the National Research Center for Disaster Prevention No.* **18,** 85-115.